Applied Ocean Research 144 (2024) 103920

Contents lists available at ScienceDirect

Applied Ocean Research

journal homepage: www.elsevier.com/locate/apor

Influence of scour and scour protection on the stiffness of monopile foundations in sand

Jann-Eike Saathoff [a,*], Norman Goldau [a], Martin Achmus [a], Alexander Schendel [b], Mario Welzel [b], Torsten Schlurmann [b]

[a] Leibniz University Hannover, Institute for Geotechnical Engineering, Germany
[b] Ludwig Franzius Institute of Hydraulic, Estuarine and Coastal Engineering, Germany

ARTICLE INFO

Keywords:
Finite-element-model, monopile
Offshore
Scour
Scour protection
Soil-structure interaction

ABSTRACT

Offshore structures are subject to cyclic effects from wind and waves, as well as altered seabed. Local and global scour can form around the foundation elements, which in turn can affect the structures' response in terms of serviceability, eigenfrequency and fatigue limit state. If a scour protection is installed, a stiffening effect is to be expected. The paper investigates the influence of local scour and scour protection on the soil-structure interaction of an exemplary monopile foundation in sandy soil with a numerical finite element model, in which the soil behaviour is modelled by the advanced HSsmall material law. With that, the effect of the depth and the geometry of a scour hole on the load deformation behaviour and in particular on the stiffness of a monopile is quantified. It is shown that the exact geometry of a conical scour hole is of minor importance for the effect on the monopile stiffness. However, scour depths of around 1.5 times the pile diameter, which are often to be considered in design, strongly reduce the stiffnesses with reduction factors of around 2.5. Furthermore, the positive influence of a scour protection layer on the soil-structure interaction is included in the comparison. First order estimates for a typical offshore configuration reveal that an installed scour protection can increase the stiffnesses of the monopile-soil system under operation considerably, mainly dependant on the thickness of the protection layer. The study exemplarily quantifies that the presence of scour protection implies an increase in structural integrity as a so far underrated added value and may actually be an effective mitigation measure for dysfunctional monopile foundations in offshore wind industry.

1. Introduction

Offshore wind turbines are essential for the desired transition from the exploitation of fossil fuels to renewable energies in the near future. The expansion of offshore wind energy represents a crucial aspect of the necessary transition in energy supply. For example, the German government has recently increased the expansion target for offshore wind energy, wherein a capacity of 30 GW is to be reached by 2030. The existing assets have a capacity of around 8 GW (German Federal Government, 2022). Various structures are available as foundations for offshore wind turbines. While the share of installed jacket structures increases, which represent the second most installed substructure in Europe (9.9 %), monopile foundations remain the most commonly used structure type (81.2 %) by far (WindEurope, 2021; Deutsche Windguard, 2022).

The installation of the offshore foundation disturbs the flow field around it, leading to locally increased bed shear stresses, initialization of sediment pick-up and sediment transport in effect. The resulting scour hole can alter the bearing behaviour of the structure by reducing the embedded length in the seabed. This imperils the stability of the entire wind turbine. For a safe and economical design of the foundation structure and its embedment depth, a reliable prediction of the expected scour depth and extent is therefore important. For slender monopiles, numerous studies and scour prediction methods are available for a wide range of hydrodynamic boundary conditions, including current (e.g., Melville and Chiew, 1999), waves (e.g., Sumer and Fredsøe, 2001) and a combined wave and current loading (e.g., Qi and Gao, 2014). However, these approaches are often based on simplified hydraulic conditions and small-scale laboratory tests. By neglecting the influence of realistic offshore wave conditions such as wave direction (Schendel et al., 2020) and tidal currents (e.g., Schendel et al., 2018) on scour development, their applicability is limited and the predicted scour depth can vary widely depending on the approach chosen and site conditions. This is particularly true for more complex foundation structures such as jackets,

* Corresponding author.

https://doi.org/10.1016/j.apor.2024.103920
Received 19 June 2023; Received in revised form 15 January 2024; Accepted 8 February 2024
Available online 12 February 2024

for which there are far fewer studies and less reliable scour prediction models and formulae. Due to these uncertainties in scour prediction, and as a cost-effective alternative to structural adjustment or extensive maintenance and monitoring campaigns, granular scour protection is typically applied around the structure to protect against scour formation. The scour protection prevents the formation of scour, but causes further costs and additional maintenance intervals are necessary. In general, granular scour protection must be designed to prevent erosion of the underlying bed material against changing hydraulic loads, while maintaining permeability to prevent the build-up of large pore pressures in the seabed and to allow rapid drainage of seepage water. In coastal and marine engineering, this is typically achieved by a multi-layer scour protection system of granular material of varying sieve distribution, consisting of a coarse protective armour layer on top and one (or more) filter layer(s) below.

In practice, the behaviour of a pile under horizontal loading is usually calculated by means of a Winkler model, i.e. a beam supported by springs. Here, scour is considered by removing the springs down to the depth of the scour holes and by reducing the vertical stresses in the soil (on which the spring stiffnesses depend) in a certain region below the scour hole (API, 2014). It is not totally clear how accurate this simplified method predicts the effect of a scour hole, since the soil type and the concrete geometry of the scour hole is not taken into account.

A few studies on the effect of scour on the bearing capacity of monopiles can be found in the literature, based on experimental tests or even numerical calculations. Investigations regarding the accurate back-calculation with a Winkler model was done by Lin et al. (2010). The results of centrifuge tests were calculated for a scour depth of 3 m using different Winkler models. By using the spring formulation according to API (2014) for the consideration of the scour effect, the displacements could be more accurately derived in comparison to the standard approach without any scour influences. Neglecting the changes of stress due to the scour hole in the Winkler approach leads to a conservative design of laterally loaded piles. Qi et al. (2016) conducted centrifuge model tests and showed that general scour has a greater effect on the pile behaviour than local scour. They proposed an approach to consider the effect of local scour in a Winkler approach. Similar results were found in the study by Li et al. (2020). This work was additionally focused on the influence of different scour shapes and different scour depths on the bearing behaviour of a monopile. Chortis et al. (2020) suggests that the distinction between local and global scour is not sufficient to adequately describe the influence of scour. It is therefore important to also consider the geometry of the local scour, as it strongly influences the properties of the Winkler model in terms of subgrade reaction and displacement in shallower soil layers.

Mayall et al. (2018) conducted experimental tests on the behaviour of a scaled monopile (diameter of 0.197 m) under consideration of scour and subsequent scour remediation measures (see also Mayall, 2019). They evaluated natural frequencies of the system and found that these were significantly affected by scour. They also found that by installing a scour protection, an increase of natural frequency occurred.

The influence of a scour protection on the lateral bearing capacity of a monopile was experimentally and numerically investigated by Askarinejad et al. (2022). The experimental setup was tested in a centrifuge and consisted of a pile with a diameter of 1.8 m and a length of 23 m (prototype dimensions) in dense sand. The scour protection was assumed to be homogeneously made of sand with a size of 5 to 7 times the diameter. The experimental tests were subsequently back-calculated with the hypoplastic constitutive model with intergranular strain. It was shown that the lateral bearing capacity can be increased up to 30 % in both dense and loose sand and that the deflection accumulation under cyclic lateral load decreased significantly. However, the study did not consider the effect of a scour protection layer on the stiffness of a monopile under operational loads. Moreover, the thickness and thus also the weight of the scour protection layer was not varied. A more detailed investigation on influence of a scour protection on the stiffness under operation is still missing.

In the design of monopile foundations, often not the bearing capacity, but the stiffness of the pile-soil system under un- and reloading, as occurring during turbine operation, is design-driving. This stiffness is important because the eigenfrequency of the overall wind turbine structure, which strongly affects the dynamic loads acting on the structure, depends on it. In particular, it must be avoided that the eigenfrequency of the wind turbine coincides with the predominating frequencies of wind and wave loads and also with the 1 P and 3 P excitation frequencies resulting from the rotation of the rotor (Schaumann et al., 2004).

To account for the compliance of the monopile in eigenfrequency determination and load calculations for the overall wind turbine system, usually a stiffness matrix for the monopile-soil system is to be defined. In general this is a 6 × 6 matrix relating the three force and three moment components to the corresponding three displacement and three rotation components at a certain pivot point. However, for a model of a monopile foundation loaded in one direction, the axial and torsional components can be neglected and only the horizontal force F, the bending moment M at seabed level and the corresponding deformations u and Q are to be considered. Hence, the monopile response can be simplified to a 2 × 2 stiffness matrix (Eq. (1)).

$$\begin{bmatrix} \Delta F \\ \Delta M \end{bmatrix} = \begin{bmatrix} \overline{K_{11}} & \overline{K_{12}} \\ K_{21} & K_{22} \end{bmatrix} \cdot \begin{bmatrix} \Delta u \\ \Delta \Theta \end{bmatrix} \tag{1}$$

The stiffness matrix entries are in general load-dependant, i.e. they depend on the maximum and minimum loads occurring in the considered situation (see e.g. Thieken 2015). In practice, this load-dependency is most often neglected, which results in constant stiffness terms.

The diagonal terms of the stiffness matrix are used here as measures of the monopile-soil stiffness. For the sake of simplicity, the terms K_{11} and K_{22} are calculated without consideration of the coupling between horizontal deformation and rotation, i.e. by applying Eqs. (2) and 3

$$K_{11} = \frac{\Delta F}{\Delta u} \tag{2}$$

$$K_{22} = \frac{\Delta M}{\Delta \theta} \tag{3}$$

Evidently, the stiffnesses are secant stiffnesses for a defined load range. It is a common concept in geotechnical engineering to assume that the un- and reloading stiffnesses of a system are similar to the initial stiffness for virgin loading (Achmus et al., 2019; Saathoff et al., 2019). Therefore, in many practical applications the un- and reloading secant stiffnesses are approximated by the initial stiffnesses K_0 of the virgin load-displacement and moment-rotation curves, respectively.

In the paper at hand, the influence of both scour holes and scour protections on the bearing behaviour of an exemplary monopile system is investigated by means of a numerical model. Thereby, the focus lies on the stiffness under un- and reloading conditions (represented by the stiffness values K_{11} and K_{22} defined above), which is often decisive for the design. The target is to exemplary quantify the effects of scour and scour protection on the monopile behaviour. With regard to scour, both the depth and the slope of the scour hole are varied and the numerical simulation results are compared to results from a simplified Winkler model approach. With regard to scour protection, thickness, width and shear strength of the protection layer are varied. The results can help, for instance, to decide if the increase of scour protection height can be an effective measure to improve the performance of a monopile which has proven to not perform satisfactorily under operation.

2. Selected reference site and metocean conditions

To provide a realistic representation of the effect of scour depth or scour protection for the selected foundation structure, an appropriate loading situation must be adopted. For the specification of metocean and

geophysical boundary conditions, a site in the German North Sea (55°25′00'' N, 4°75′00'' E) was selected. This site was also chosen as a reference in the collaborative research centre CRC 1463 (Schuster et al., 2021). The water depth at the reference site is assumed to 48.2 m. However, as this site has not yet been developed, the availability of field data is limited. Changes of mean sea level (MSL) for different return periods were thus adopted from the nearby Alpha Ventus wind farm (DOTI, 2007). Depth-averaged current velocities and wave parameters (significant wave height H_s and peak period T_p) were obtained for the reference site from the CoastDat-2 TRIM hindcast dataset (Gaslikova et Weisse, 2013). Extreme wave conditions for several return periods were computed by means of an extreme value analysis.

Considering the large water depth, it is expected that the depth-averaged current has a greater impact on the scour development than waves. Therefore, in addition to two storm events with return periods of 10 years and 100 years, a scenario with current-only conditions was selected as a load combination for the scour estimation. The load combinations are based on the DNV guidelines (DNV-OS-C101, 2021) and are relatively conservative, as extreme storm events are combined with the maximum set-down of the water level. While a return period of one year was selected for the current-only load case, a 50-year return period for the current velocities (extreme current model) was chosen for the other two load combinations. For the current-only load case, the water depth was set to MSL, whereas for the other two load cases the MSL was reduced by the lowest seawater level (LSWL) for the corresponding return periods.

Table 1 summarizes the hydrodynamic conditions for the three load combinations. Here, the maximum orbital flow velocity U_w was determined by the parametric approach of Roulund et al. (2016) for linear, irregular waves. The Keulegan-Carpenter-number (KC-number) is calculated as $U_w T_p/D$ with D as the pile diameter, T_p as the peak wave period and the current-to-wave velocity ratio as $U_{cw} = U_c / U_c + U_w$.

The fictitious reference monopile, chosen for this investigation, has a diameter of $D = 8$ m with an embedded length of $L = 24$ m (i.e. a length-to-diameter ratio of 3) and an assumed load eccentricity of $e = 40$ m. This is a typical large-diameter monopile system, since in current projects the L/D ratios tend to rather small values around 3 and may in future projects become even smaller (Burd et al., 2020). Negro et al. (2017) evaluated monopile designs with pile diameters mainly between 3 m and 6 m and reported L/D-values between 3.5 and 9.5. However, they also showed that the L/D-ratio by trend becomes the smaller, the greater the pile diameter is. Therefore, the choice of $L/D = 3$ for a monopile with $D = 8$ m in competent soil seems suitable and at least not unrealistic. The wall thickness is set to be constantly $t = 0.078$ m. The dimensions as well as the used symbols in this work are shown in Fig. 1. Fig. 1(a) shows the case for no scour, Fig. 1(b) shows the case for a scour mitigation and Fig. 1 (c, d) the case for local (LS) and global (GS) scour. Global scour is defined here as the erosion of soil of thickness S over the entire area of interest (quasi-infinite width), corresponding to a general subsidence of the seabed.

In the following, the maximum scour depth to be expected is determined and also a scour protection layout is derived, in order to define basic values for the subsequent parametric study. The considered subsoil is a narrow-graded fine sand, which is typical North Sea sand. The grain size distribution of the material is depicted in Fig. 2. The coefficients of uniformity and curvature are $C_U = 1.5$ and $C_C = 1.0$, respectively. The relevant grain size diameters are $d_{10} = 0.175$ mm, $d_{30} = 0.200$ mm and $d_{50} = 0.235$ mm.

3. Scour depth estimation

Given the large water depth, it is assumed that the scour process is largely driven by the tidal current. Therefore, scour prediction approaches for steady current loading are used to estimate a representative scour depth. Numerous approaches are available for estimating the scour depth at monopiles, which often result in a variety of different scour depths. To minimize uncertainties, the expected scour depth is therefore estimated with several approaches to determine an average value. The individual approaches are, however, only briefly mentioned and the assumptions of input parameters are summarized hereafter. For the prediction of the scour development under current-only conditions, the well-known approaches listed in Table 2 were chosen. For the approach of Breusers et al. (1977), a factor of 2 has been chosen to consider the influence of the water depth and the critical flow velocity was calculated with the approach described in Soulsby (1997). In the HEC-18 equation (Richardson et Davis, 2001), a correction factor for the bed condition of $K_3 = 1.15$ for small dunes was used. The definition of a critical flow velocity as given by Sheppard et al. (2014) was used for the corresponding scour prediction approach. All other shape and attack angle factors were chosen according to a circular pile. In the process, only the mean grain size d_{50} is used for the derivation of scour depth.

The final scour prediction depths are depicted in Table 2. The equations used in the calculations are collected in the appendix to this paper. The average value of 10.58 m is used in the following as the possible maximum value. Considering the diameter of the pile of 8 m, the derived scour depth is similar to the suggested one by the DNV and API. The slope of the scour hole α is usually assumed to be dependant on the internal friction angle φ' of the soil.

4. Scour protection layout

If the estimated scour depths exceed defined threshold values, scour mitigation measures by means of scour protections can be used. The calculation of the required armour layer stone size for a granular scour protection followed the static design approach by De Vos et al. (2011). While current-induced flow is the main driver of the continuous development of scour, large waves locally induced during storms result in temporary bed-shear stresses that are considerably greater than the current-induced ones. The dimensioning of armour layer stones is based on the comparison between the acting bed-shear stresses with the critical shear stresses of the stones, which represent their resistance to displacement. The required armour layer stone diameters result in a median diameter $d_{50} = 0.367$ m for the load combination with a 10-year return period and a $d_{50} = 0.504$ m for the load case with a 100-year return period. The fact that the stone diameters turn out to be small despite the extreme hydraulic boundary conditions is due to the large water depth, which significantly attenuates the wave-induced flow reaching the top of the scour protection. Based on the calculated armour

Table 1
Hydrodynamic site condition for the selected reference for current-only conditions and a 10- as well 100-year-return period.

	Significant wave height H_s	Peak wave period T_p	Current flow velocity U_c	Water depth d	maximum orbital velocity U_m	Keulegan-Carpenter number KC	Current-to-wave velocity ratio U_{cw}
Load case	[m]	[s]	[m/s]	[m]	[m/s]	[-]	[-]
Current only	–	–	1.05	48.2	–	–	–
Storm 10 yr	11.25	11.89	1.35	46.3	0.87	1.29	0.61
Storm 100 yr	12.96	12.76	1.35	46.0	1.15	1.83	0.54

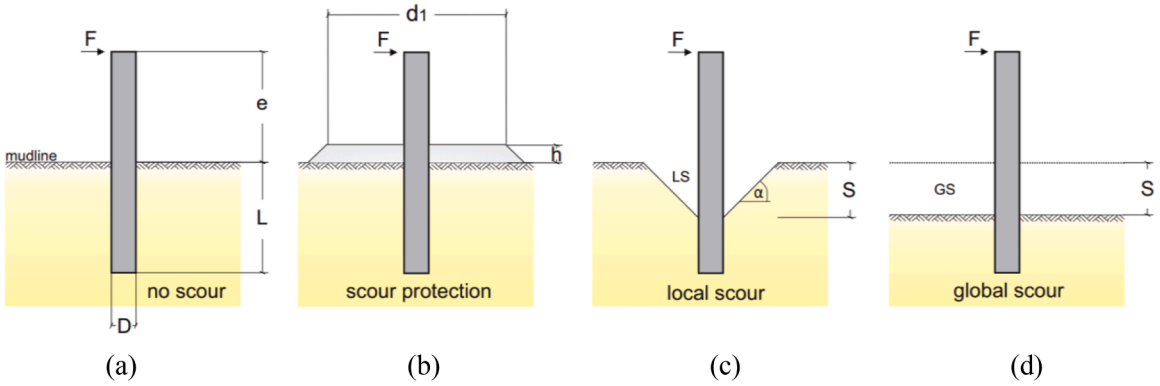

Fig. 1. Definition of calculation models: no scour, scour protection, local scour and global scour.

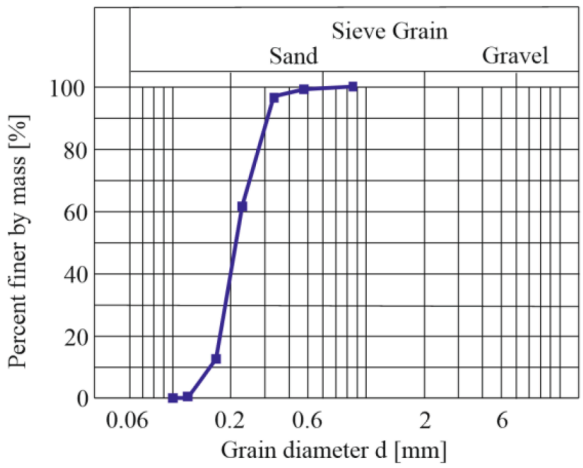

Fig. 2. Grain size distribution of reference soil.

layer stone sizes, commercially available gradings for a conventional 3-layer scour protection setup were selected (Table 3). For all gradings, a stone density of 2,650 kg/m^3 is assumed. The armour layer is assumed to be 1.0 m high, the upper filter layer 0.4 m and the lower filter layer 0.3 m. These are typical layer thicknesses, which results in a total scour protection height of 1.7 m.

The armour layer is given a spatial extent of 5D, which represents a standard extent that has been frequently used in previous studies or was applied in the field (Chavez et al., 2019; de Vos et al., 2011). For the underlying filter layers, an extension of 6D is chosen. As this is not of relevance in this study, filter stability has not been confirmed for the chosen scour protection setup, but might be assumed given the 1–200 mm material for the lower filter layer. With the chosen design and extent of scour protection, edge scour which can occur at the outer end of the scour protection (Petersen et al., 2015) should normally be prevented or should at least have a relatively small effect on the monopile stiffness.

5. Scour consideration with winkler model

When designing monopiles, it is common to use a subgrade reaction model (spring-supported beam, Winkler model) to calculate the bearing behaviour. In this model, the soil is represented by springs with non-linear load-displacement relationships (Fig. 3(a)). This approach is termed p-y method and is stated in the current Offshore Guidelines (API 2014; DNV-OS-J101 2014). Originally, the method was developed and calibrated for flexible, small-diameter piles. Based on research by Cox et al. (1974) and O'Neill et Murchison (1983), a hyperbolic tangent function was utilized to characterize the p-y relation for piles in sandy soils. The p-y curve is defined by the maximum bedding resistance p_u and the initial stiffness of the p-y curve E_{py} (cf. Fig. 3(a)). These depth-dependant values are computed using the buoyant unit weight of the sandy soil and the angle of internal friction.

The approach needs to be modified for the application to large-diameter monopiles to take the actual bearing behaviour into consideration, which is more comparable to the behaviour of a rigid pile. In recent years, various approaches have been developed to better account for the load-bearing behaviour of monopiles (e.g. Soerensen et al. 2012, Kallehave et al., 2012, Kirsch et al., 2014, Thieken et al., 2015). For the calculations conducted here, the approach according to Thieken et al. (2015) was used, since this approach was proven to realistically predict the load-bearing behaviour of a monopile over the entire range of loads and deformations. This approach was developed for sand soils by calibration with the results of a numerical simulation model with an advanced elasto-plastic material law for the soil. It accounts for the stress-dependency of soil stiffness and also for the increased stiffness of soils at small strain levels, which is particularly important with regard to initial stiffness calculations.

In p-y models, the p-y curve (i.e. the spring characteristic) for a

Table 2
Scour depth predictions around a monopile with $D = 8$ m for current-only conditions.

Load combinations	Breusers et al. (1977) [m]	HEC 18, Richardson and Davis (2001) [m]	Sheppard et al. (2014) [m]	Zanke (1982) [m]	Sumer et al. (1992) - DNVGL [m]	Average [m]
Current only 1yr	16.00	9.37	6.54	10.61	10.40	10.58

Table 3
Selected gradings and layer thicknesses for a 3-layer scour protection setup.

Load combinations	Armour layer [kg]	Armour layer thickness [m]	Upper filter layer [kg]	Upper filter layer thickness [m]	Lower filter layer [mm]	Lower filter layer thickness [m]
Storm 10 yr	40–200	0.8	5–40	0.3	1–200	0.3
Storm 100 yr	60–300	1.0	10–60	0.4	1–200	0.3

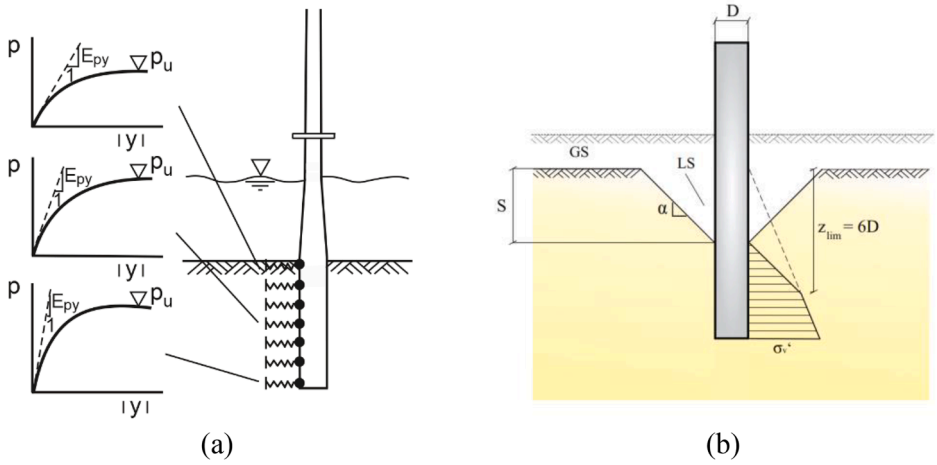

Fig. 3. Subgrade reaction model (a) and vertical effective stress distribution considered in the Winkler model to consider scour (schematic following API (2014)) (b).

considered depth depends on the vertical effective stress acting in that depth. To account for a scour hole, the springs down to the scour depth are removed. The distribution of vertical stress below the scour hole can be approximated with the approach presented in API (2014). Herein, it is assumed that the vertical stress increases linear with depth down to a limiting depth z_{lim} where the stress for the case without scour hole is reached. The resulting bi-linear stress distribution is depicted in Fig. 3 (b). According to the API, a typical limiting depth is 6 times the pile diameter. This depth is seen as representative to consider the reduction of stresses in the bedding area.

The Winkler model was calculated with the in-house pile design software IGtHPile (cf. Terceros et al., 2015). The input parameters for the p-y approach according to Thieken et al. (2015) are given in Table 4. The parameters were aligned with the parameter sets given in Table 5 for soil and equivalent scour protection used in the numerical simulation model.

Fig. 4 shows the calculated moment-rotation curve at the mudline for the case of no scour (black line). The ultimate pile capacity was derived based on the load-displacement curve to 28.5 MN at a displacement of 0.8 m (0.1 D). The corresponding ultimate moment is 1140 MNm and the ultimate rotation is 0.046 rad. Different scour depths up to 10.5 m were evaluated with the p-y model (blue lines in Fig. 4). The results clearly show the great effect of a scour hole on both pile capacity and stiffness. At the maximum considered scour of 10.5 m, the residual pile loading capacity is less than 20 % of the pile without scour. This makes clear why for monopiles usually scour protection measures are used.

Additionally, scour protection layers with thicknesses of 1 m, 1.7 m and 3 m were considered in the Winkler model (red curves). A significant beneficial contribution of the different scour protection heights can be identified. However, it must be noted that in the Winkler model the limited width of the scour protection layers cannot be accounted. Hence, it is to be expected that the stiffening effect will be overestimated.

In a Winkler model, several idealizations are made. In particular, the stress changes in the soil due to a scour hole must be estimated and the limited width of the scour protection layer cannot be considered. For a more accurate analysis, a finite element calculation is necessary in which also a sophisticated constitutive model for the sand may be used. The results of the Winkler models – and in particular the initial stiffnesses – will be used for comparison with the numerical simulation results.

Table 4
Soil parameters for soil and scour protection layer used for the p-y approach according to Thieken et al. (2015).

Parameter	Unit	Soil	Scour protection
Buoyant unit weight γ'	[kN/m^3]	10.3	10.5
Angle of internal friction φ'	[°]	38	40
Poisson's ratio υ_{ur}	[1]	0.25	0.25
Reference stress p_{ref}	[kN/m^2]	100	100
Stiffness parameter λ	[1]	0.50	0.40
Reference stiffness $E_{oed,ref}$	[MN/m^2]	90	90
Reference shear modulus $G_{0,ref}$	[MN/m^2]	126	111

Table 5
Soil parameters of the reference system.

Parameter	Unit	Soil	Armour layer	Lower / Upper filter layer	Equivalent scour protection
Buoyant unit weight γ'	[kN/m^3]	10.3	10.0	11.0	10.5
Cohesion c'	[kN/m^2]	0.1	0.1	0.1	0.1
Angle of internal friction φ'	[°]	38	42	35	40
Angle of dilatancy ψ	[°]	8	12	5	10
Shear strain $\gamma_{0.7}$	[1]	0.0001	0.0001	0.0001	0.0001
Poisson's ratio υ_{ur}	[1]	0.23	0.25	0.25	0.25
Reference stress p_{ref}	[kN/m^2]	100	100	100	100
Earth pressure coefficient at rest k_0	[1]	0.38	0.33	0.43	0.36
Stiffness parameter λ	[1]	0.50	0.40	0.40	0.40
Reference stiffness $E_{oed,ref}$	[MN/m^2]	70	90	50	70
Reference stiffness $E_{50,ref}$	[MN/m^2]	70	90	50	70
Reference stiffness $E_{ur,ref}$	[MN/m^2]	210	270	150	210
Reference shear modulus $G_{0,ref}$	[MN/m^2]	126	134	92	111
Dynamic stiffness quotient E_{sd}/E_s	[1]	4.8	4.5	5.5	4.8

6. Numerical model

Because the Winkler model cannot capture all effects influencing the soil-structure interaction due to positive or negative scour, a finite

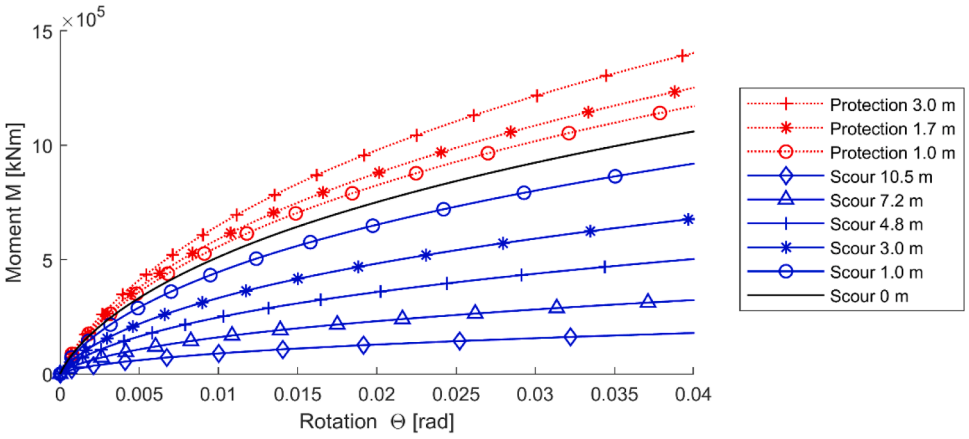

Fig. 4. Moment-rotation curve for different scour depths and for the case with scour protection calculated with the Winkler model.

element model was established. The numerical analyses were performed with the finite element (FE) software Plaxis3D (Bentley, 2022). Fig. 5 exemplary shows typical numerical models used in this study, once with local scour and once with scour protection.

Due to the symmetry conditions of the loading and the pile, only one half of the system was modelled to save computation time. In the scope of preliminary analyses, the size of the discretized soil domain and the fineness of the finite element discretization ensuring an accurate numerical solution were identified. The analyses showed that a model with a width of 25D in loading direction, a depth of 2 L and a breadth of 6 D perpendicular to the loading direction is great enough to avoid any significant boundary effects on the calculation results. 10-node wedge elements (cf. Bentley Systems, 2022) were used in the discretization of the soil volume. Up to a distance from the monopile of 1.5 D in horizontal direction and 2 D in vertical direction, a very fine discretization was applied (cf. Fig. 5). A typical edge length of an element in the refined area was around 0.12 D, whereas outside this area the edge lengths were around 0.6 D to 0.7 D.

To find a suitable discretization ensuring accurate results, the mesh fineness was systematically varied (herein keeping the ratios of element

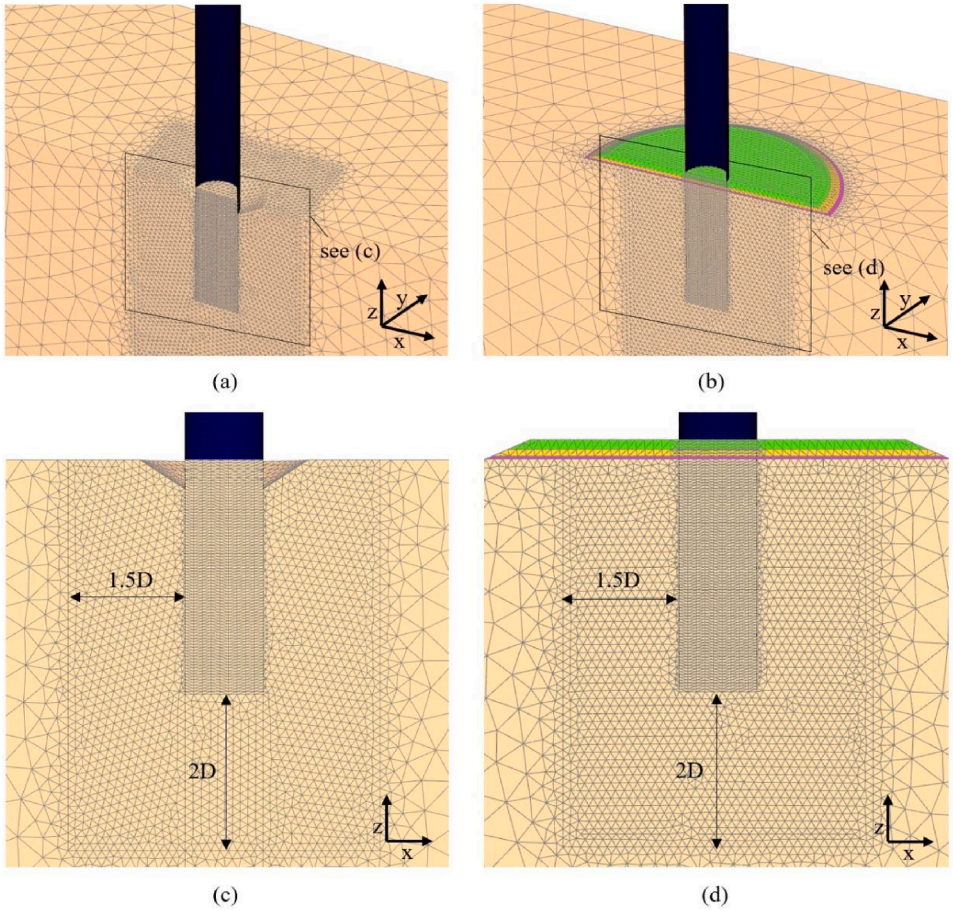

Fig. 5. Numerical reference model with symmetric local scour of 3 m (a, c) and layered scour protection with a total height of 1.7 m and a maximum extension of 6D (b, d). In (b) and (d), the layers of the scour protection are marked by different colors.

sizes in the refined area and outside almost constant). As an example of the conducted convergence study, Fig. 6 shows the lateral displacement of the monopile at mudline dependant on the overall number of elements. The final model was discretized with 185,182 elements for the case of the system without scour considered in Fig. 6. For the system with a scour protection of 1.7 m height, 209,881 elements were used. With these numbers of elements, the absolute error in the calculated displacements remained below 1.5 % (cf. Fig. 6), which is considered acceptable for the purpose of this study.

The monopile is modelled tubular and open-ended. For the steel material, linear-elastic behaviour was assumed with a Young's modulus $E = 2.1 \cdot 10^8$ kN/m^2, a Poisson's ratio $\nu = 0.27$ and a steel unit weight $\gamma_s =$ 68 kN/m^3. For modelling the contact behaviour between steel and soil, elasto-plastic interface elements are attached to the monopile. The maximum shear stress in the contact surface τ_{max} results from the product of the horizontal stress σ_H and the tangent of the contact friction angle $\delta = 2/3\ \varphi$'.

First, the initial stress state in the soil was calculated by assuming that the ratio of horizontal to vertical effective stress is given by $k_0 = 1 -$ sin φ'. Subsequently, the monopile is installed in a wished-in-place procedure, i.e. soil elements are replaced by steel elements where the pile is located. The scour protection (or the scour hole) is considered after the pile was installed. Subsequently, the lateral and moment loading is applied. The maximum lateral load was chosen to be 6 MN, which is approximately 20 % of the bearing capacity at 0.1D obtained with the Winkler model.

An advanced material law is required to take the non-linear soil behaviour at small strains and un- and reloading situations into account. The Hardening soil small (HSsmall) model (Benz, 2007) was chosen as a constitutive model since it can consider the higher stiffness for small strains and distinguishes between stiffnesses under primary loading and un- and reloading. The HSsmall model is an upgraded version of the sophisticated Hardening Soil model (HS) according to Schanz (1998), which is an elasto-plastic model with isotropic hardening and also enables the consideration of stress-dependant soil stiffness. The stiffness parameters $E_{oed,ref}$, $E_{50,ref}$, $E_{ur,ref}$ and λ (cf. Table 5) can be derived based on triaxial tests and an oedometric compression test. Governed by two parameters $G_{0,ref}$ and $\gamma_{0.7}$, the model also accounts for the dependence of stiffness on shear strain, applying the approach of Santos et Correia (2001) (Fig. 7):

$$\frac{G}{G_0} = \frac{1}{1 + 0.385\ \frac{\gamma}{\gamma_{0.7}}} \tag{4}$$

Here, the reference shear strain $\gamma_{0.7}$ corresponds to the shear strain at which the soil stiffness is decreased to 72.2 % concerning the dynamic shear modulus G_0.

For the simulations described in this paper, the parameters given in Table 5 were applied. The parameters given for the soil are typical for a dense sand. The scour protection consists of an armour layer placed above lower and upper filter layers. Also a parameter set for an equivalent scour protection is given. It was shown that using this parameter set for the whole scour protection instead of explicitly modelling the different layers of the scour protection leads to very similar results. Therefore, the equivalent scour protection parameters where used in the parameter study.

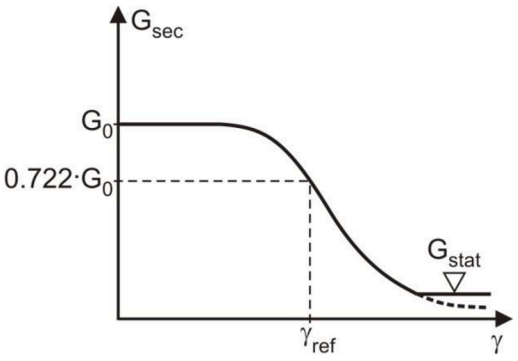

Fig. 7. Relation between shear modulus and shear strain according to Santos et Correia (2001).

7. General results

For the reference system, scour holes with 1 m, 2 m and 3 m depth and a slope of $\alpha = \varphi' = 38°$ were considered. The scour was modelled by deleting soil elements present in the desired scour hole.

In a first step, the effect of different temporal sequences of scour development and load application was investigated. The black curve in Fig. 8(a) shows the moment-rotation curve for a sequential application of loading and scour. First, the load of 6 MN (moment $M = 240$ MNm) and following complete unloading was applied to the system without scour. Then, development of a scour hole of 1 m was simulated and re- and unloading was performed. Afterwards, the scour hole was extended to 2 m depth and re- and unloading was performed, etc. The blue lines in Fig. 8(a) show the results gained with the non-sequential approach. Here, before any load application the scour hole development of 1 m, 2 m or 3 m was simulated and then un- and reloading was performed. As evident from Fig. 8, the non-sequential and the sequential calculations lead to almost identical results regarding the maximum rotation under loading and the plastic rotation after unloading (Fig. 8(b)). Also the secant stiffness for un- and reloading are almost identical. Hence, the temporal sequence of scour development is of minor importance. In the following, only the non-sequential procedure will be used.

Fig. 9 compares the monopile responses to primary loading and un- and reloading for the cases without scour, with scour depths of 3.0 m and 10.5 m and with consideration of a scour protection of 1.7 m thickness. Evidently, either a scour hole or a scour protection have a great effect on the stiffness of the monopile. The designed scour protection almost halves the pile rotation under the considered load and

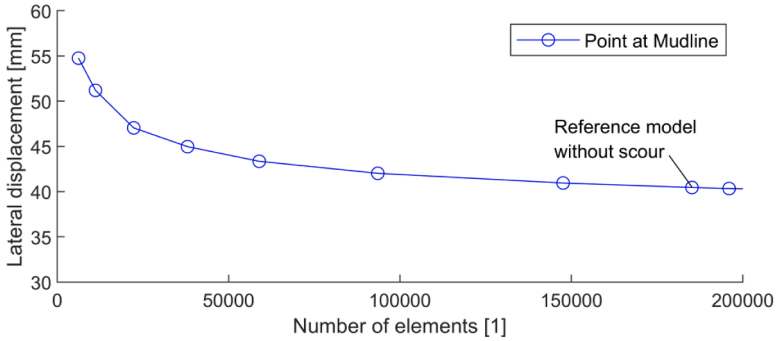

Fig. 6. Exemplary results of the convergence study: Lateral displacement of the monopile at mudline dependant on the total number of elements.

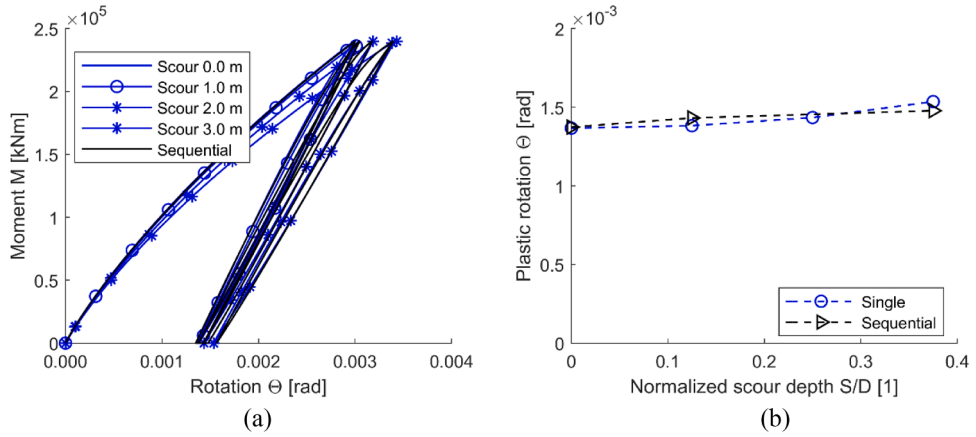

Fig. 8. Comparison of the effect of sequential and non-sequential scour evolution on the moment-rotation curve.

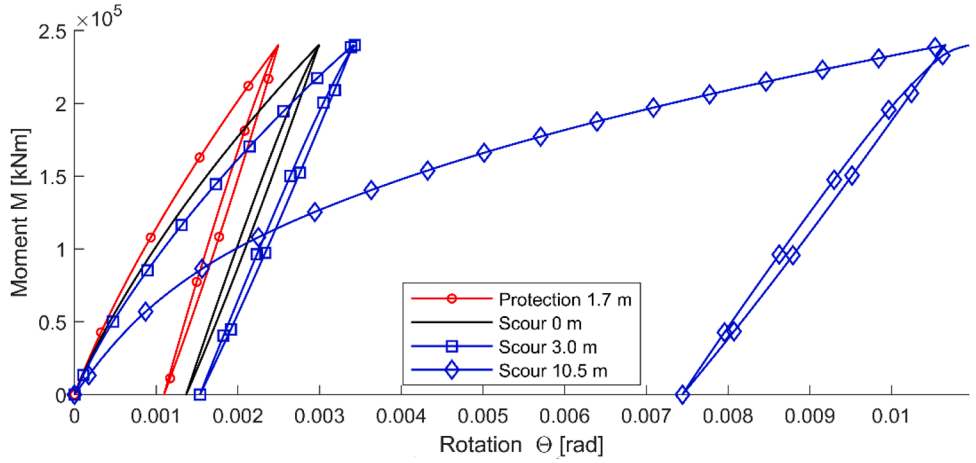

Fig. 9. Moment-rotation curve for derived scour depth and scour protection.

also affects the un- and reloading stiffness considerably. As to be expected, a scour hole strongly degrades the pile stiffness.

The degradation can be quantified by comparing the (secant) stiffness matrix entries for the case of no scour and a scour depth of 3 m. Fig. 10 shows the stiffnesses calculated with Eqs. (2) and 3. For the primary loading case, the nonlinearity of the load-deflection and moment-rotation curves manifests in a decrease of secant stiffness with increasing deflection or rotation. The red dashed line in Fig. 10 gives the secant stiffness for the full un- and reloading hysteresis curve, which is in this case slightly smaller than the initial value for primary loading.

In the following parametric study, either the secant stiffness entries for the un- and reloading curve or the initial stiffness entries for the primary loading curve are considered in order to analyse the effects of scour or scour protection on the monopile behaviour. Thereby, for

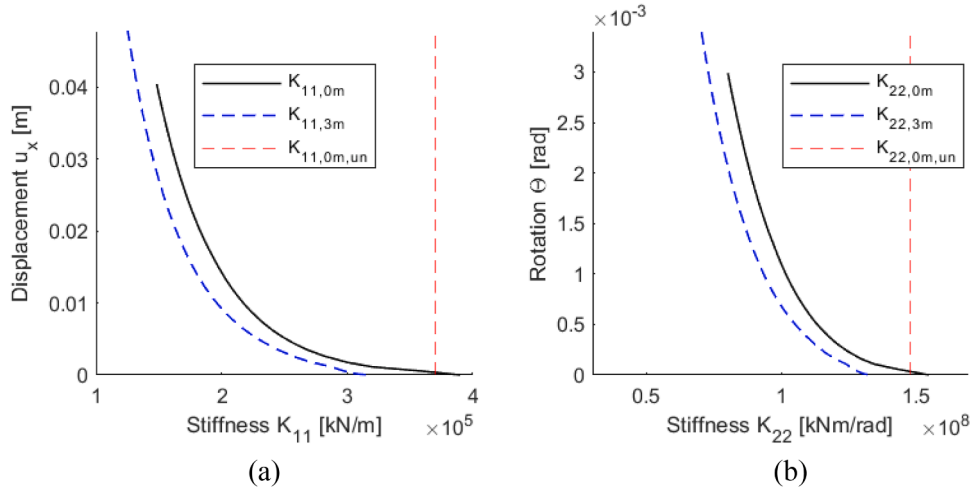

Fig. 10. Stiffness matrix entries for reference system with no scour in comparison with the case of a scour depth of 3 m.

practical reasons the initial stiffnesses are determined as secant stiffnesses for a very small deformation, viz. at 1 mm pile displacement.

8. Parameter study

8.1. Consideration of scour hole geometry

The discussion of the numerical results in the previous chapter proved the significant negative effect of the local scour holes on the monopile's response for the reference system. To further quantify the effect, the influence of different scour geometries will be shown. Fig. 11 (a) shows the variation of the scour hole inclination α. For the reference system, $\alpha = \varphi' = 38°$ was assumed. This value was varied now between 20° and 38° For the investigation of the effect of scour depth ($S = 1$ m / 2 m /3 m), the scour hole inclination was set equal – as in the reference case – to the angle of internal friction (Fig. 11(b)).

The moment-rotation curves for different scour depths with the assumption of $\alpha = \varphi' = 38°$ have already been presented in Fig. 9. Fig. 12 shows the moment-rotation curves for scour depths of 1.0 m and 3.0 m together with a quantitative comparison of rotational stiffnesses for the considered scour depths. A scour depth of 3.0 m leads to considerable stiffness decreases of 10 % compared to the case without scour regarding lateral and moment stiffness. For a scour depth of 1.0 m, the stiffness decreases are moderate (2.5 %). The relation between degree of softening and scour depths is obviously non-linear.

Fig. 13(a) depicts the moment-rotation curves with different scour hole inclinations for a scour depth of 3.0 m. The increase in displacement between the case with the maximum slope inclination of $\alpha = 38°$ and a gentle slope inclination of $\alpha = 20°$ is approximately 5 %. Thus, the different scour inclinations have only a marginal effect. This analysis was only done for the 3 m scour case and may be less pronounced for a scour depth of 1.0 m. Fig. 13(b) graphically depicts the effect of scour hole inclination on the rotational secant stiffness for un- and reloading. As to be expected, the stiffness increases with increasing inclination, although the dependency is not very pronounced. However, the stiffness for a global scour of 3 m depth, which is theoretically equivalent with a scour hole inclination of $\alpha = 0°$, is considerably smaller. This value is also depicted in Fig. 13(b). Compared to the case with $\alpha = 38°$, the rotational stiffness decreases by about 11 %. The results clearly show that the exact inclination of a scour hole is of minor importance, but global and local scour must definitely be distinguished.

8.2. Consideration of scour protection

The favourable effect of the designed scour protection with a thickness of 1.7 m has already been presented in Fig. 9. Here, the three-layered structure of the scour protection (as shown in Fig. 15 left) was modelled with the material properties given in Table 5. Fig. 14 shows the moment-rotation curves for scour protection heights between 0.5 m and 3.0 m compared to the reference curve for the case without scour protection. Evidently, the stiffness increases significantly with increasing scour protection height. Moreover, the higher the scour protection layer is, the smaller is the plastic deformation of the monopile, i.e. the remaining rotation after full unloading.

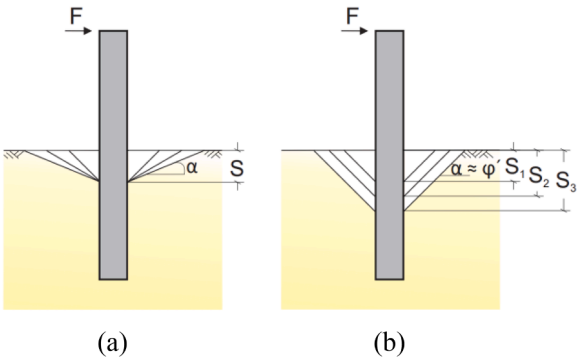

Fig. 11. Different scour hole inclinations (a) and scour depths (b).

The stiffening effect of a scour protection layer can be caused by the stiffness and shear strength of the layer itself and by the increase of stresses in the subsoil due to the own weight of the layer. In order to analyse which effect predominates, further calculations were conducted. Fig. 15 shows four types of scour protection modelling. Type (1) is a layered scour protection consisting of three soil layers (lower/ upper filter and armour layer), as planned in reality. In a second calculation (type 2), the scour protection is idealized as a homogeneous layer of one material (equivalent scour protection, cf. Table 5). Type (3) analyses the separate influence of the dead weight of the scour protection. Therefore, the equivalent vertical stress was applied at the subsoil surface, which means that the stiffnesses and shear strengths of the scour protection layers are neglected and the additional resistances result only from an increased vertical stress in the subsoil. In the fourth calculation (type 4), the homogeneous layer is assumed to have an infinite length. Comparing type 4 and type 2 results, the effect of the limited width of the scour protection layer can be identified.

Fig. 16 shows the effects of the four different modelling types in terms of the differences in the un- and reloading stiffness values K_{11} with respect to the stiffness calculated for the reference case (Fig. 15 left, type 1). Evidently, modelling of a three-layered or an equivalent one-layered scour protection layer (type 2) makes almost no difference. Therefore, the latter approach was applied in the following parametric study. Neglecting the limited spatial extent of the scour protection layer (type 4) instead of considering $d_1 = 5D$ (40 m) (cf. Fig. 15) overestimates the stiffness by about 7 % and is therefore not a suitable approach. Instead, neglecting the stiffness and shear strength of the scour protection layers (type 3) leads to an underestimation of monopile stiffness of about 6 % compared to the reference case type 1. The stiffness for the type 1 case is approx. 30 % greater than the stiffness of the monopile without scour protection (see Fig. 17). This indicates that the increase of vertical stress in the subsoil by the scour protection layer is the predominating effect for stiffness increase.

8.3. Comparison of stiffnesses

In the following presentations, the height of the scour protection layer is considered as a negative scour depth. Fig. 17 shows the influence of positive and negative scour depths on the initial stiffness values K_{11} and K_{22}. As a reference, the case without scour or scour protection is used. Both results from the Winkler model (p-y model) and from the numerical simulation are presented. The effect of a scour hole on the stiffnesses is evident from the figure. According to the numerical simulation results, both stiffness entries are affected in the same manner. For small scour depths, the p-y approach gives similar results, but for scour depths greater than about 0.2D, it significantly overestimates the stiffness decrease.

A scour protection considerably increases both stiffness values. Interestingly, the increase of the horizontal stiffness is greater than of the rotational stiffness. In comparison to the finite element results, the horizontal stiffness is larger in the case of the p-y approach but smaller for the moment component. It should also be noted that the p-y approach according to Thieken (2015) was, amongst others, calibrated regarding the initial stiffness from Plaxis calculations. For a different p-y model the estimation accuracy may vary. In order to realistically account for the effect of a scour protection layer, in general finite element simulations seem to be necessary.

Fig. 18 shows the effect of scour depth on stiffnesses in terms of initial stiffness for primary loading and un- and reloading stiffness, determined with the numerical model. Evidently, for the case of scour holes (positive values of S/D) initial stiffnesses and un- and reloading stiffnesses are almost identical. This does not hold for the case of scour

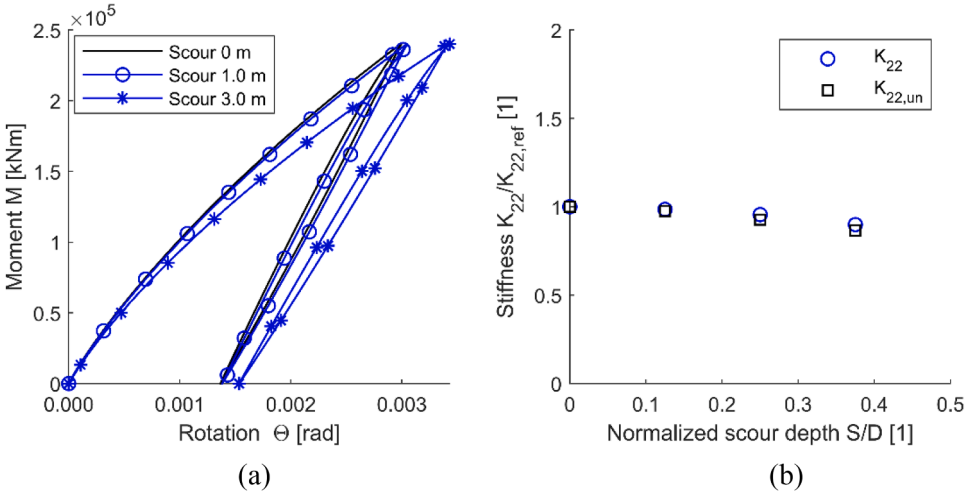

Fig. 12. Moment-rotation curves (a) and relative rotational stiffnesses for different scour depths (b).

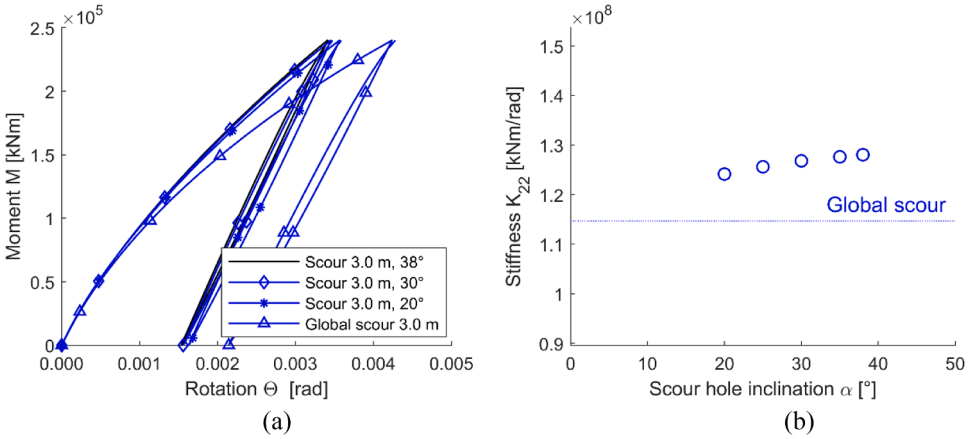

Fig. 13. Comparison of the moment-rotation curve (a) and resulting initial secant hysteresis stiffness as well as stiffness for 3 m global scour in dotted blue (b).

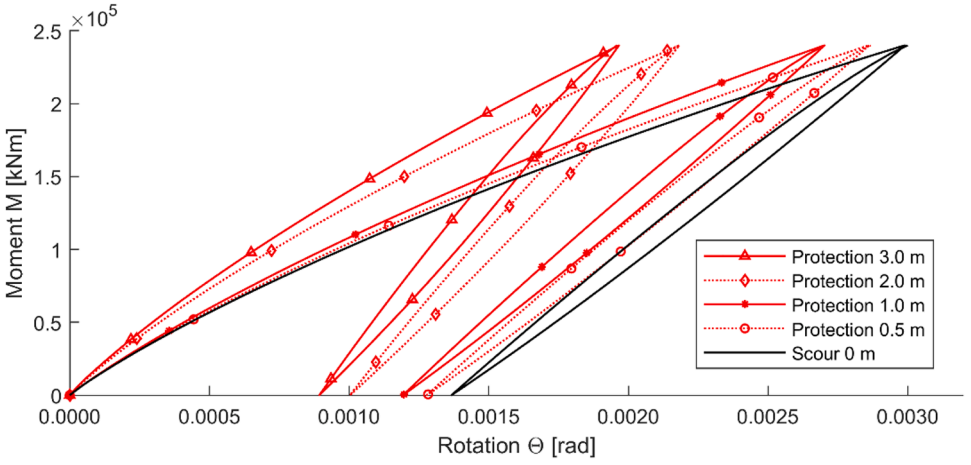

Fig. 14. Moment-rotation curve for the case with three-layered scour protection.

protection. Here, the un- and reloading stiffnesses are much greater affected than the initial stiffnesses.

Both Figs. 17 and 18 clearly show a very favourable effect of a scour protection layer on monopile stiffness. Interestingly, the rate of stiffness increase with increasing scour protection height is much greater than the rate of stiffness decrease with increasing scour hole depth. The results indicate that accounting for the effect of a scour protection layer might make sense to achieve an economic design.

The results presented so far apply for a subsoil consisting of dense sand. Additional calculation series were conducted for medium dense and very dense sand, respectively. The applied soil properties are shown in Table 6. The same scour protection properties as for the case with

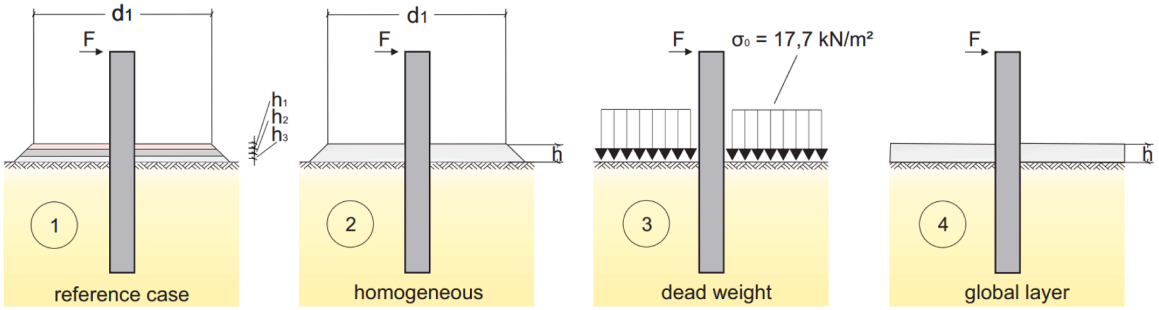

Fig. 15. Four different modelling types to consider the scour protection.

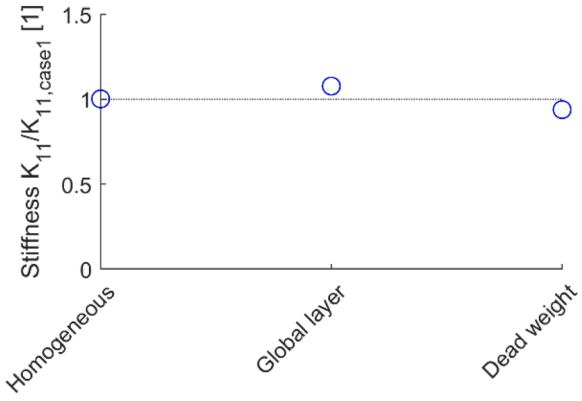

Fig. 16. Effect of different modelling approaches of scour protection on hysteretic horizontal stiffness for a scour protection height of 1.7 m with respect to the reference case 1.

dense sand were used. The inclination α of the scour hole was chosen equal to the angle of internal friction φ'. Fig. 19 shows the effects of scour and scour protection on the un- and reloading stiffness K_{11} for the three relative densities considered. In comparison with the reference case, the looser soil results in a slightly larger stiffness increase due to a scour protection layer, whereas a denser soil generates a smaller stiffness increase. This behaviour is however only pronounced for the largest investigated scour protection height of 3 m. In most cases, there is only a marginal effect on the derived horizontal stiffness component from un- and reloading between the different relative densities.

9. Discussion

The results presented clearly show the considerable influence of scour and a scour protection layer on the bearing behaviour and, in particular, on the stiffness (which is decisive for the behaviour in operation) of a monopile in sandy soil. As expected, even relatively shallow scour depths result in a significant reduction of both stiffness and bearing capacity. The application of different approaches for scour depth prediction led to an average scour depth of 10.58 m for the considered case with a monopile of 8 m diameter. The numerical simulation results showed that for such a scour depth, a stiffness decrease compared to the case without scour is about 50 %. This is the reason why scour protection is usually provided for large-diameter monopiles in practice.

Interestingly, a scour protection layer leads to an appreciable increase in monopile stiffness that may render as added value of structural integrity. For the designed scour protection with a layer thickness of 1.7 m ($S/D = -0.21$), the calculated increase in stiffness is about 30 % (see Fig. 18). If the layer thickness is doubled, a stiffness increase of about 50 % can be expected. This clearly indicates that an increase of the scour protection layer could be an effective measure to improve the stiffness of sandy soil as an enhancement of structural bearing capacity of an already installed monopile. Furthermore, a very important result is that the stiffening effect of a scour protection layer is mainly caused by its weight, i.e. by increasing the stresses in the subsoil, and only to a little amount by its stiffness and shear strength. This means that the effect is still present when a gap has formed between the pile and the armour material, e.g. due to a rearrangement of individual stones of the scour protection layer during a severe storm.

Askarinejad et al. (2022) also showed the positive effect of scour protection on bearing capacity. For a pile with a diameter of 1.8 m in loose and dense sand, they showed that the bearing capacity under an

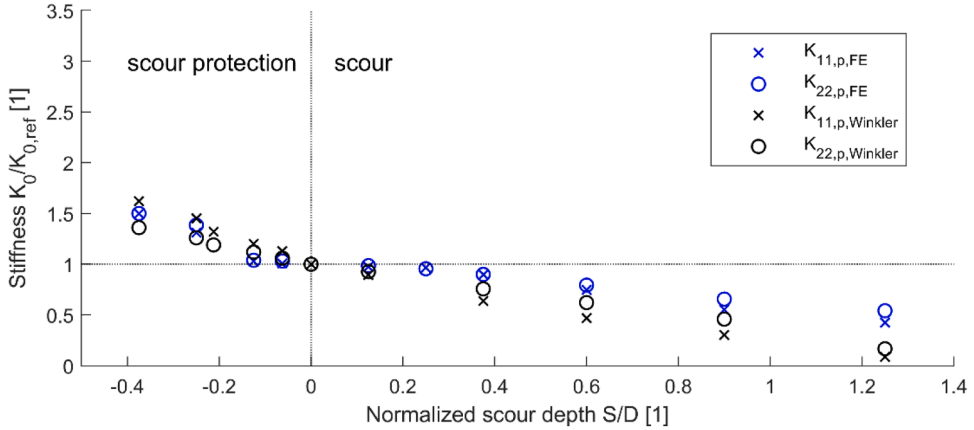

Fig. 17. Results of finite element simulation and p-y model for different scour depths as well as consideration of scour protection on initial stiffness for primary loading (secant stiffness at 1 mm displacement).

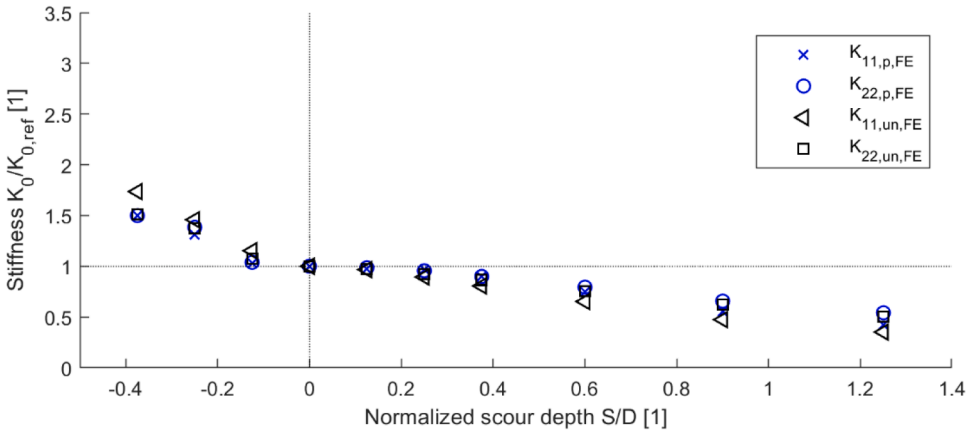

Fig. 18. Results of finite element simulation for different scour depths as well as consideration of scour protection on initial stiffness for primary loading and un- and reloading stiffness.

Table 6
Further soil parameters of the study with two different relative densities as comparative calculation.

Parameter	Unit	Sand, medium dense	Sand, very dense
Buoyant unit weight γ'	[kN/m^3]	10.3	10.7
Void ratio e_{init}	[1]	0.65	0.60
Cohesion c'	[kN/m^2]	0.1	0.1
Angle of internal friction φ'	[°]	33	42
Angle of dilatancy ψ	[°]	3	12
Shear strain $\gamma_{0.7}$	[1]	0.0001	0.0001
Poisson's ratio υ_{ur}	[1]	0.25	0.20
Reference stress p_{ref}	[kN/m^2]	100	100
Earth pressure coefficient at rest k_0	[1]	0.46	0.33
Stiffness parameter λ	[1]	0.65	0.50
Reference stiffness $E_{oed,ref}$	[MN/m^2]	30	100
Reference stiffness $E_{50,ref}$	[MN/m^2]	30	100
Reference stiffness $E_{ur,ref}$	[MN/m^2]	90	300
Reference shear modulus $G_{0,ref}$	[MN/m^2]	62.0	150.4
Dynamic stiffness quotient E_{sd}/E_s	[1]	6.2	4.0

eccentricity of 12.7 $D = 22.86$ m increases by about 30 % when a scour protection layer with an effective surcharge pressure of 15 kN/m^3 is applied. They also found that the favourable effect is mainly due to the own weight of the protection layer and the effect of stiffness and shear strength can be neglected. In that sense, the results presented here generally confirm the results of Askarinejad et al. (2022). Additionally, the general validity for real monopile dimensions ($D = 8$ m) could be confirmed and the effect of varying thicknesses of a scour protection layer on the operational stiffness of the system could be quantified. For the same thickness of the protection layer as assumed by Askarinejad et al. (2022), the stiffness increase obtained for the large monopile diameter is around 25 % and thus slightly smaller than reported by Askarinejad et al. (2022).

It should be noted that the results were obtained for a typical monopile geometry ($D = 8$ m, $L/D = 3$) selected as an academic example to analyse the additional bearing capacity and to showcase the actually added value of structural integrity. Although it can be assumed that similar relative stiffness changes will result for monopiles with deviating D and L/D values, this requires verification. In this respect, the study presented quantifies the influence of scour and scour protection layers only as an example in the sense of a fundamental investigation.

In the parameter study, the eccentricity of the load with respect to the sea bottom was also assumed to be $e = 40$ m and was initially not varied. In an additional series of numerical simulations, the identical monopile systems in dense sand were investigated under a horizontal load with an eccentricity of $e = 80$ m. Fig. 20 shows the stiffness changes determined for this case. Comparison with Fig. 18 shows that even with a significantly larger eccentricity, the relative stiffness changes are very similar to those for the reference case. This is also valid for the relative positions regarding the primary stiffness, the un- and reloading stiffness of the hysteresis from finite element calculations as well as the primary

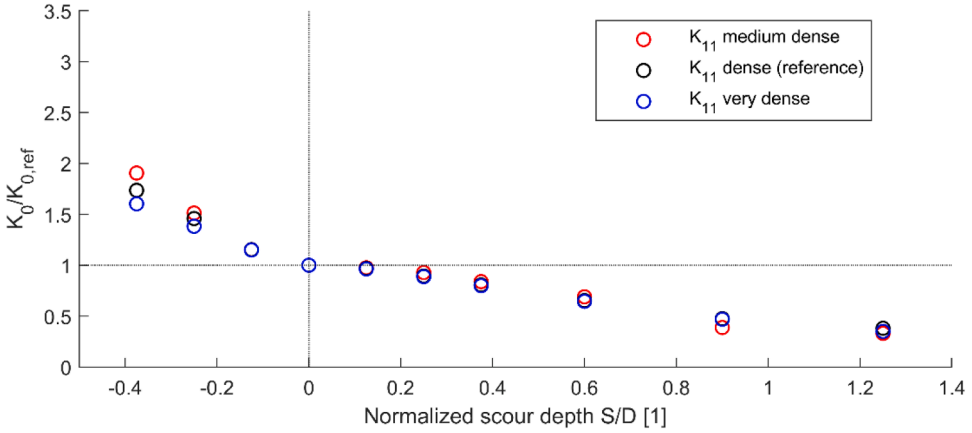

Fig. 19. Results of finite element simulation for positive and negative scour depth on un- and reloading stiffness for different relative densities.

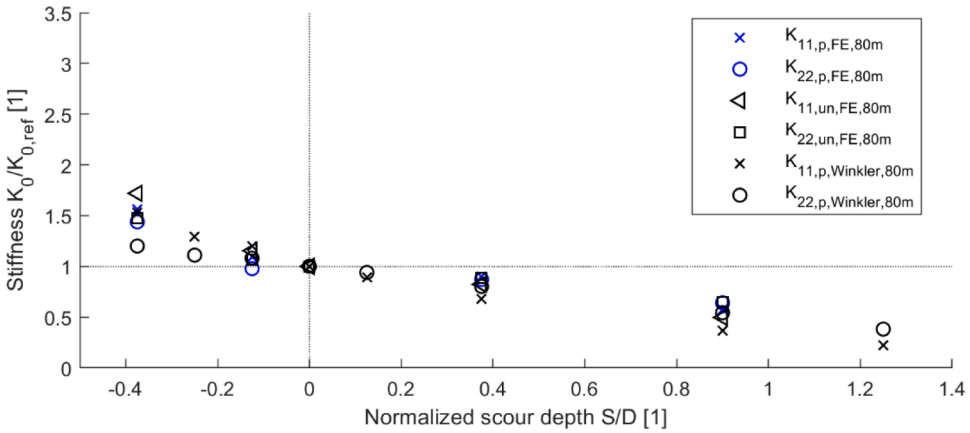

Fig. 20. Results of finite element simulation for different scour depths as well as consideration of scour protection on monopile stiffnesses with an eccentricity of $e =$ 80 m.

stiffness derived from the Winkler model.

10. Conclusions

Due to maritime conditions, scour may develop during the lifetime of an offshore structure. For large-diameter monopile foundations, large scour depths may occur and considerably affect the foundation performance during wind turbine operation. Therefore, in most cases a scour protection is designed to avoid scour and its unfavourable effect. The favourable effect of a scour protection on the monopile performance is usually not considered in the design.

In the presented study, the effect both of scour holes and scour protection layers were investigated and quantified for an exemplary monopile with a diameter of $D = 8$ m and an embedded length of 24 m in sand soil. The following main conclusions can be drawn from the results:

- With p-y models, the influence of scour can be realistically estimated only for small scour depths up to about 0.2D. For larger scour depths, the simplified approaches give results that differ significantly from those of a numerical simulation. Regarding the scour protection, the p-y approach according to Thieken (2015) gives results that agree fairly well with the derived stiffnesses from numerical simulations. However, there is a slight overestimation regarding the horizontal stiffness component.
- The numerical simulations have confirmed that the un- and reloading stiffness, which are relevant for the investigation of operating conditions, can be approximately represented by the initial stiffness of the primary loading curve. Both stiffnesses are similarly reduced by a scour. The initial stiffness yields similar results to the un- and reloading stiffness.
- Small changes in inclination of the scour hole (20° up to 38°) have only a minor influence on the initial stiffness (deviations of at maximum 5 %).
- A scour protection layer of a given height has a much stronger positive effect on the stiffness (up to 50 % stiffness increase when the height of the protection layer is doubled from 1.7 m to 3.4 m) than a scour with the depth of 1.7 m, which has a negative effect (decrease by 20 %). However, a maximum scour depth typically to be accounted for in a design reveals a strongly negative effect on the stiffness, which decreases by about 60 %.
- In the numerical simulations, a similar effect on the stiffness was obtained when considering only the stress resulting from the dead weight of the scour protection. This observation is significant as it implies that the effect persists even when a gap has formed between the pile and the armour material.
- The influence of the relative density on relative stiffness changes does not seem to be very pronounced, except for larger scour protections heights. It was also proven that similar relative stiffness changes apply for different eccentricities of the horizontal load.

It must be pointed out that the results gained and the conclusions drawn apply to a typical, but exemplary case and the general validity must be verified by further investigations. However, the results show that consideration of scour protection in the design can contribute significantly to economic efficiency. In cases of insufficient stiffness of an existing monopile, increasing the scour protection thickness can be an effective improvement measure. However, increasing the thickness of the scour protection can have some adverse effects which may affect the stability of the scour protection against hydraulic loading. Chiew (1995) conducted a series of experiments focused on evaluating the stability of scour protection systems with varying thicknesses and extents. In these tests, the top of the scour protection was installed flush with the seabed and the failure of the protection under steady, unidirectional flow was determined. The results of these tests indicate a trend of enhanced stability with increasing scour protection thickness. Petersen et al. (2015) carried out an extensive test series on the development of edge scour around a scour protection system. Their findings emphasized the crucial role played by the thickness-to-width ratio of the scour protection system in determining the equilibrium scour depth. In general, the incoming flow is disrupted and deflected by the scour protection. With increasing thickness, the disruption and acceleration of the flow intensify, and wake vortices become more pronounced. As a result, edge scour depths, in particular on the downstream side of the protection, increase.

In the present study, only a specific pile diameter and a specific L/D-ratio with different relative densities of sand soil was investigated. In future research projects, alternative pile diameters and L/D-ratios could be considered to investigate the influence on stiffness changes. It is also desirable to consider cases with stratified soil conditions to approach a more realistic scenario.

CRediT authorship contribution statement

Jann-Eike Saathoff: Conceptualization, Data curation, Investigation, Methodology, Validation, Visualization, Writing – original draft, Writing – review & editing. **Norman Goldau:** Conceptualization, Data curation, Investigation, Methodology, Validation, Visualization, Writing – original draft, Writing – review & editing. **Martin Achmus:** Conceptualization, Methodology, Supervision, Writing – original draft, Writing – review & editing. **Alexander Schendel:** Conceptualization, Investigation, Methodology, Writing – original draft, Writing – review & editing. **Mario Welzel:** Conceptualization, Methodology, Writing –

original draft, Writing – review & editing. **Torsten Schlurmann:** Conceptualization, Methodology, Writing – original draft, Writing – review & editing.

Declaration of competing interest

The authors declare that they have no known competing financial interests or personal relationships that could have appeared to influence the work reported in this paper.

Data availability

Data will be made available on request.

Acknowledgements

The investigations reported were funded by the Deutsche Forschungsgemeinschaft (DFG, German Research Foundation) - SFB1463 – 434502799. The support is gratefully acknowledged.

APPENDIX

Selected approaches for prediction of scour depth S around a pile in steady current conditions:

Breusers et al. (1977):

$$S = Df_1(2\tanh(d/D))f_2f_3$$

$$f_1 = \begin{cases} 0\ for\ U_c/U_{cr} \le 0.5 \\ 2\ (U_c/U_{cr}) - 1 \text{ for } 0.5\ < U_c/U_{cr} \le 1.0 \\ 1\ for\ U_c/U_{cr} > 1.0 \end{cases}$$

With d as the water depth, f_1 as the correction factor for the flow regime, f_2 as the shape correction factor ($f_2 = 1.0$ for circular piles), f_3 as the correction factor for the angle of attach ($f_3 = 1$ for circular piles), U_c as the current flow velocity and U_{cr} as the critical flow velocity of the sediment, which was calculated with the approach described in Soulsby (1997).

HEC 18, Richardson and Davis (2001):

$$S = 2dK_1K_2K_3(D/d)^{0.65}Fr^{0.43}$$

$$Fr = \frac{U_C}{\sqrt{gd}}$$

With g as the acceleration of gravity (9.81 m/s^2), Fr as the Froude Number upstream of the pile, K_1 as the correction factor for pile nose shape ($K_1 = 1$ for circular piles), K_2 as the correction factor for the angle of attack ($K_2 = 1$ for circular piles) and K_3 as the correction factor for bed condition, which was set to $K_3 = 1.15$ to represent small dunes.

Sheppard et al. (2014):

$$\frac{S}{a} = 2.5f_1f_2f_3 \text{ for } 0.4\ \le \frac{U_c}{U_{cr}} < 1.0$$

$$\frac{S}{a} = f_1\left[2.2\left(\frac{\frac{U_c}{U_{cr}} - 1}{\frac{U_p}{U_{cr}} - 1}\right) + 2.5f_3\left(\frac{\frac{U_p}{U_{cr}} - \frac{U_c}{U_{cr}}}{\frac{U_p}{U_{cr}} - 1}\right)\right] \text{ for } 1.0\ \le \frac{U_c}{U_{cr}} \le \frac{U_p}{U_{cr}}$$

$$\frac{S}{a} = 2.2f_1 \text{ for } \frac{U_c}{U_{cr}} > \frac{U_p}{U_{cr}}$$

$$f_1 = \tanh\left[(d/a)^{0.4}\right]$$

$$f_2 = \left\{1 - 1.2\left[\ln\left(\frac{U_c}{U_{cr}}\right)\right]^2\right\}$$

$$f_3 = \left[\frac{\left(\frac{a}{D_{50}}\right)}{0.4\left(\frac{a}{D_{50}}\right)^{1.2} + 10.6\left(\frac{a}{D_{50}}\right)^{-0.13}}\right]$$

$$U_p = \begin{cases} U_{p1}\ for\ U_{p1} \ge U_{p2} \\ U_{p2}\ for\ U_{p2}\ > U_{p1} \end{cases}$$

$$U_{p1} = 5U_c$$

$$U_{p2} = 0.6\sqrt{gd}$$

Where a is the effective diameter of the pile $= K_sa_p$, with K_s as the shape factor ($K_s = 1$ for circular piles) and a_p as the projected width of the pile. U_{cr} as the critical flow velocity of the sediment was calculated with the approach described in Sheppard et al. (2014).

Zanke et al. (1982):

$$S = 2.5D\left(1 - 0.5\frac{U_{cr}}{U_c}\right)$$

DNVGL, Sumer et al. (1992):

$$S = 1.3D$$

References

Achmus, M., Thieken, K., Saathoff, J.E., Terceros, M., Albiker, J., 2019. Un- and reloading stiffness of monopile foundations in sand. Appl. Ocean Res. 84, 62–83. https://doi.org/10.1016/j.apor.2019.01.001.

ANSI/API RP 2GEO, 2014. Geotechnical and foundation design considerations: ANSI/API recommended practice 2GEO; ISO 19901-4:2003 (modified). Petroleum and Natural Gas Industries - Specific requirements For Offshore Structures Part 4. American Petroleum Institute and American National Standards Institute, Washington, DC. Recommended practice.

Askarinejad, A., Wang, H., Chortis, G., Gavin, K., 2022. Influence of scour protection layers on the lateral response of monopile in dense sand. Ocean Eng. 244, 110377 https://doi.org/10.1016/j.oceaneng.2021.110377.

Bentley Systems. Plaxis software. 2022.

Benz, T., 2007. Small-strain stiffness of soils and its numerical consequences. Universität Stuttgart. PhD thesis. https://www.igs.uni-stuttgart.de/dokumente/Mitteilungen/55_Benz.pdf (Retrieved 2023-01-09).

Breusers, H.N.C., Nicollet, G., Shen, H.W., 1977. Local scour around cylindrical piers. J. Hydraulic Res. 15 (3), 211–252. https://doi.org/10.1080/00221687709499645.

Burd, H.J., Abadie, C.N., Byrne, B.W., Houlsby, G.T., Martin, C.M., McAdam, R.A., Jardine, R.J., Pedro, A.M.G., Potts, D.M., Taborda, D.M.G., Zdravkovic, L., Andrade, M.P., 2020. Application of the PISA design model to monopiles embedded in layered soils. Geotechnique 70 (11), 1067–1082.

Chavez, C.E.A., Stratigaki, V., Wu, M., Troch, P., Schendel, A., Welzel, M., et al., 2019. Large-scale experiments to improve monopile scour protection design adapted to climate change - The PROTEUS project. Energies. (Basel) 12 (9), 1709. https://doi.org/10.3390/en12091709.

Chiew, Y.M., 1995. Mechanics of riprap failure at bridge piers. J. Hydraulic Eng. 121 (9), 635–643. https://doi.org/10.1061/(ASCE)0733-9429(1995)121:9(635).

Chortis, G., Askarinejad, A., Prendergast, L.J., Li, Q., Gavin, K., 2020. Influence of scour depth and type on p-y curves for monopiles in sand under monotonic lateral loading in a geotechnical centrifuge. Ocean Eng. 197, 106838 https://doi.org/10.1016/j.oceaneng.2019.106838.

Cox, W.R., Reese L.C., .and Grubbs, B.R. (1974). Field testing of laterally loaded piles in sand. Paper presented at the Offshore Technology Conference. URL https://doi.org/10.4043/2079-MS.

Deutsche Windguard (2022). Status of offshore wind energy development in Germany, First Half of 2022.

De Vos, L., De Rouck, J., Troch, P., Frigaard, P., 2011. Empirical design of scour protections around monopile foundations. Static Approach. Coastal Eng. 58, 540–553. https://doi.org/10.1016/j.coastaleng.2011.02.001.

DNV-OS-C101 (2021). Design of offshore steel structures, general - LRFD method.

DNV-OS-J101 (2014). Design of Offshore Wind Turbine Structures.

DOTI G.M.B.H. (2007). Borkum West - Hydrographische Standortbedingungen.

Gaslikova, L., Weisse, R. (2013). coastDat-2 TRIM-NP-2d tide-surge North Sea. World Data Center for Climate (WDCC) at DKRZ. https://doi.org/10.1594/WDCC/coastDat-2_TRIM-NP-2d.

German federal government (2022). More wind energy at sea. https://www.bundesregierung.de/breg-de/themen/klimaschutz/windenergie-auf-see-gesetz-2022968, Retrieved 01.12.2022.

Kallehave, D., LeBlanc Thilsted, C., Liingaard M.A. (2012). Modification of the API p-y formulation of initial stiffness of sand. Proceedings of the 7th International Conference Offshore Site Investigation and Geotechnics, pp. 465–472.

Kirsch, F., Richter, T., Coronel, M. (2014). Geotechnische Aspekte bei der Gründungsbemessung von Offshore-Windenergieanlagen auf Monopfählen mit sehr großen Durchmessern. Stahlbau Spezial 2014 - Erneuerbare Energien, pp. 61–67, in German.

Mayall, R.O., 2019. Monopile response to scour and scour protection. University of Oxford. PhD thesis. https://ora.ox.ac.uk/objects/uuid:2886ac08-c59e-409d-8d60-6724443d8d1a/.

Mayall, R.O., Byrne, B.W., Burd, H.J., McAdam, R.A. (2018). Modelling of foundation response to scour and scour protection for offshore wind turbine structures. Scour and Erosion IX – Proceedings of the 9th International Conference on Scour and Erosion (ICSE 2018), pp. 405–413.

Melville, B.W., Chiew, Y.M., 1999. Time scale for local scour at bridge piers. J. Hydraulic Eng. 125, 59–65. https://doi.org/10.1061/(ASCE)0733-9429(1999)125:1(59.

Li, Q., Askarinejad, A., Gavin, K., 2020. The impact of scour on the lateral resistance of wind turbine monopiles: an experimental study. Canadian Geotechnical J. 37, 1008–1014. https://doi.org/10.1139/cgj-2020-0219.

Lin, C., Bennet, C., Han, J., Parsons, R.L., 2010. Scour effects on the response of laterally loaded piles considering stress history of sand. J. Comp. Geotechnics 37, 1008–1014. https://doi.org/10.1016/j.compgeo.2010.08.009.

Negro, V., Lopez-Gutierrez, J.S., Esteban, M.D., Alberdi, P., Imaz, M., Serraclara, J.M., 2017. Monopiles in offshore wind: preliminary estimate of main dimensions. Ocean Eng. 133 (2017), 253–261. https://doi.org/10.1016/j.oceaneng.2017.02.011.

O'Neill, M.W., Murchison, J.M., 1983. An Evaluation of P-Y Relationships in Sands. University of Houston.

Petersen, T.U., Sumer, B.M., Fredsoe, J., Raaijmakers, T.C., Schouten, J.J., 2015. Edge scour at scour protections around piles in the marine environment — Laboratory and field investigation. Coast. Eng. 106 (2015), 42–72.

Qi, W.G., Gao, F.P., 2014. Physical modelling of local scour development around a large-diameter monopile in combined waves and current. Coast. Eng. 83, 72–81. https://doi.org/10.1016/j.coastaleng.2013.10.007.

Qi, W.G., Gao, F.P., Randolph, M.F., Lehane, B.M., 2016. Scour effects on p-y curves for shallowly embedded piles in sand. Géotechnique 66 (8), 648–660.

Richardson, E.V., Davis, S..R., 2001. Evaluation Scour At Bridges. Federal Highway Administration, U.S. Dept. of Transportation, Washington, D.C.. Tech. rep. Publication No. FHwA NHI 01-001.

Roulund, A., Sutherland, J., Todd, D. and Sterner, J. (2016). Parametric equations for Shields parameter and wave orbital velocity in combined current and irregular waves. ICSE 2016 (8th International Conference on Scour and Erosion), 12–15 September 2016, Oxford, UK.

Saathoff, J.E., Thieken, K. and Achmus, M. (2019). Evaluation of un- and reloading stiffness and damping of monopile foundations in sand soils, 29th Int. Ocean and Polar Engineering Conference (ISOPE), Honolulu/USA, June 16-21.

Santos, J.A., Correia, A.G., (2001). Reference threshold shear strain of soil and its application to obtain a unique strain-dependent shear modulus curve l. Proceedings of the 15th International Conference on Soil Mechanics and Geotechnical Engineering, pp. 267–270.

Schanz, T., 1998. Zur Modellierung des Mechanischen Verhaltens von Reibungsmaterialien. *Habilitation*. University of Stuttgart.

Schaumann, P., Kleineidam, P., Wilke, F., 2004. Fatique design bei offshore-windenergieanlagen. Stahlbau 73 (9), 716–726. https://doi.org/10.1002/stab.200490175. VolumeIssue.

Schendel, A., Hildebrandt, A., Goseberg, N., Schlurmann, T., 2018. Processes and evolution of scour around a monopile induced by tidal currents. Coast. Eng. 139, 65–84. https://doi.org/10.1016/j.coastaleng.2018.05.004.

Schendel, A., Welzel, M., Schlurmann, T., Hsu, T.W., 2020. Scour around a monopile induced by directionally spread irregular waves in combination with oblique currents. Coast. Eng. 161, 103751 https://doi.org/10.1016/j.coastaleng.2020.103751, 2020 Jul 21.

Schuster, D., Hente, C., Hübler, C., Rolfes, R., 2021. Integrierte Entwurfs- und Betriebsmethodik für Offshore-Megastrukturen. Bautechnik 98 (8), 563–570. https://doi.org/10.1002/bate.202100044.

Sheppard, D.M., Melville, B., Demir, H., 2014. Evaluation of existing equations for local scour at bridge piers. J. Hydraulic Eng. 140 https://doi.org/10.1061/(ASCE)HY.1943-7900.0000800.

Sørensen, S.P.H., 2012. Soil-structure interaction for non-slender large-diameter offshore monopoles. Aalborg University Denmark, Department of Civil Engineering. PhD Thesis.

Soulsby, R., 1997. Dynamics of Marine sands: A manual For Practical Applications. Thomas Telford Publications, London.

Sumer, Fredsøe, 2001. Wave scour around a large vertical circular cylinder. J. Waterway Port, Coastal, Ocean Eng. 127 (3), 125–134. https://doi.org/10.1061/(ASCE)0733-950X(2001)127:3(125.

Sumer, B.M., Fredsøe, J., Christiansen, N., 1992. Scour around vertical pile in waves. J. Waterw.. Port, Coast. Ocean Eng. 118 (1), 15–31. https://doi.org/10.1061/(ASCE)0733-950X(1992)118:1(15).

Terceros, M., Schmoor, K.A., Thieken, K., 2015. IGtHPile version 4 software and reference manual. Leibniz University of Hannover, Institute for Geotechnical Engineering, Hannover, Germany.

Thieken, K., 2015. Geotechnical design aspects of foundations for offshore wind energy converters. Leibniz University of Hannover. PhD Thesis.

Thieken, K., Achmus, M. and Lemke, K. (2015). A new static p-y approach for piles with arbitrary dimensions in sand, Geotechnik, 02 December, Issue 38 (4), pp. 267–288.

WindEurope, 2021. Offshore Wind in Europe: key trends and statistics 2020. Tech. Rep. 2021.

Zanke, U. (1982). Grundlagen Der Sedimentbewegung. Ed. by U. Zanke. (In German). Springer-Verlag - Berlin - Heidelberg - New York.